

Oracle Bone Inscription Recognition Based on Isometric Mapping Algorithm

Ping Xie, Hao Xu

School of Mathematics and Information, China West Normal University, Nanchong, China

Email: xieping@stu.cwnu.edu.cn, xhheqiao@126.com

How to cite this paper: Xie, P. and Xu, H. (2025) Oracle Bone Inscription Recognition Based on Isometric Mapping Algorithm. *Applied Mathematics*, 16, 321-337. <https://doi.org/10.4236/am.2025.164016>

Received: February 28, 2025

Accepted: April 11, 2025

Published: April 14, 2025

Copyright © 2025 by author(s) and Scientific Research Publishing Inc.

This work is licensed under the Creative Commons Attribution International License (CC BY 4.0).

<http://creativecommons.org/licenses/by/4.0/>



Open Access

Abstract

In this paper, the Isometric Mapping (ISOMAP) algorithm is applied to recognize oracle bone inscription images. First, the sample set undergoes denoising and size normalization as preprocessing steps. Subsequently, a gray-value matrix is extracted from the images as their feature representation. The ISOMAP algorithm is then implemented to obtain a low-dimensional embedding of the sample set. Following this, the classification is performed by selecting the label corresponding to the nearest neighbor category with the highest frequency around the test sample. By optimizing the parameters of the ϵ -neighborhood and N , the recognition accuracy reaches 93.3%. Finally, the performance of ISOMAP is compared with other manifold learning algorithms. Experimental results demonstrate that ISOMAP achieves a higher average recognition rate and lower computational time compared to its counterparts. Therefore, ISOMAP algorithm proves to be an effective tool for oracle bone inscription recognition.

Keywords

Oracle Bone Inscription, Manifold Learning, Image Recognition, ISOMAP Algorithm

1. Introduction

Oracle bone inscription is the earliest pictographic script in China, which possess a significant historical and cultural value [1]. This ancient Chinese script of ancient originated in Shang Dynasty [2] acted as a medium for divination and event documentation. It etched onto turtle shells or animal bones [3]. Hence, it serves as an invaluable resource for studying the history of the Shang Dynasty. It also plays a pivotal role in researching the genesis and evolution of Chinese characters, aiding the understanding of ancient Chinese history. The majority of these

inscriptions were unearthed at Yinxu in Anyang, located in Henan province. So far, there are about 154,000 pieces of bone and turtle fragments have been excavated, and about 4500 single characters have been discovered on them [4]. They are characterized by many irregular characters and complex structures. These inscriptions are carved on tortoise shells as shown in **Figure 1** [5].

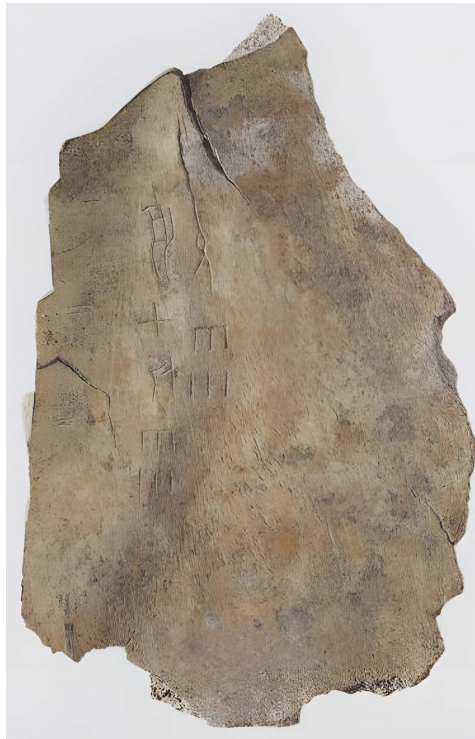


Figure 1. A tortoise shell with tortoise bone scripts unearthed in the Yinxu of Anyang, Henan Province.

Due to the specialties of oracle bone inscriptions as carriers, the existing textual information on bones may gradually disappear over time. However, it is pleasant that with the development of computer technology becoming increasingly mature, this information has been digitally preserved. This also provides a basic condition for computer recognition of inscriptions [6]. Nowadays, technology of image recognition has been widely used in various fields, and image recognition of the inscription has become an important research field.

Figure 2 [5] shows another form of preservation of inscriptions in the form of rubbings.

From the above, although it can be seen that the processed topology retains the information of inscriptions, a certain amount of noise is brought. Due to the addition of noise, it causes a certain impact on computer recognition and brings great challenges to computer recognition of images. A few decades ago, a graph theory of oracle identification method was used in [7] [8]. In recent years, researchers have proposed some methods to recognize oracle bone inscription. A complex Convolutional Neural Networks (CNN [9]) model was used to recognize

it by Liu *et al.* in [10]. The method of Deep Learning was used by Meng *et al.* in [11]. A coding recognition technique based it was proposed by Chen *et al.* in [12]. A kind-based SVM recognition technique was used by Liu *et al.* in [13]. The database of OBC306 was set up by Huang *et al.* in [3], which has brought great convenience to recognize it. However, the previous several methods require to expend great resources, and the over-generalization of images leads to the final recognition accuracy which is not particularly high. So, we need to find more efficient identification technology and accelerate the development to recognize it. The ISOMAP algorithm in manifold learning can keep the Euclidean distance of sample points in high-dimensional space well after dimensionality reduction. So we're going to introduce how to use ISOMAP algorithm to recognize images of oracle bone inscription.



Figure 2. An oracle bone inscription preserved in the form of a rubbing.

2. Feature Extraction and Dimensionality Reduction

In **Figure 3**, it displays that the entire process of recognition, where I stands for preprocessed image, II represents low-dimensional representation of sample set, III refers to result of recognition. The process can be divided into five steps, the specific steps are (1)-(5).

- (1) Selection of sample set. The sample set is selected from dataset.
- (2) Image preprocessing. We apply the technology of image processing to denoise and normalize the size of each image.
- (3) Classification of images. The sample set of denoised was divided into training set and test set. Some images in the sample set are randomly selected as test set, and the remaining images are used as train set.

(4) Dimensionality reduction. The training set and test set are vectorized, then they are formed into a new matrix. Next, this matrix is centralized, and finally entered into the ISOMAP algorithm, a matrix of low dimension was obtained.

(5) Recognition. The label corresponding to the minimum distance from the maximum number of the same category near the measured point is selected as the final recognition result.

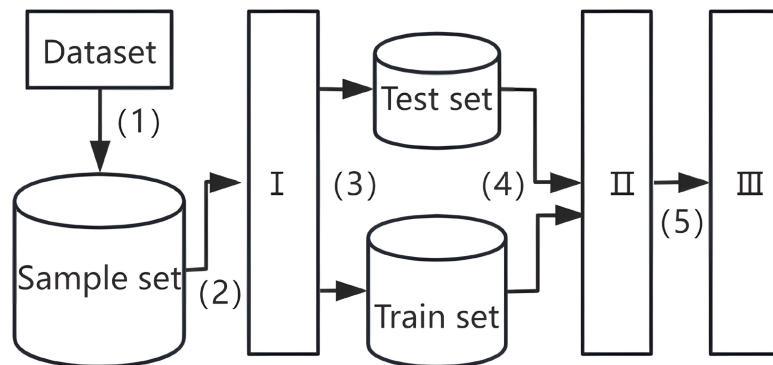


Figure 3. Recognition process of using ISOMAP algorithm.

2.1. Dataset Process

1) Dataset Preprocessing: Since there are different kinds of noises in the images in the sample set, if they are not removed, the recognition results of this experiment will be greatly affected. Each image is denoised by the method of gray value adjustment. It refers to gray value less than a value $a \times 255$ as noise, and changes their values to 0, greater than another value $b \times 255$ as script information of images, and changes them to 255, where a and b a value between 0 and 1. After the images were denoised, we do size normalization of these images. Finally, all of images were saved in size of $n \times n$.

2) Feature Extraction: A very important step of image recognition is how to extract the features of the image in recognition. In computer vision, the gray value of an image is a basic and key feature. Gray value is a way to strip away the color information and only retain and process the brightness information. In a grayscale image, each pixel has a value between 0 and 255. The gray value of the image can describe the contour information of the object in the image, and the gray value around different objects in the image will have a significant difference. Therefore, the gray value of the image can be used as the feature of the image.

As all of images have been denoised and size normalized after preprocessing, the gray values of an image form a matrix. In this paper, the gray value matrix of each image is used as characters for recognition. The gray value of each image is splintered into a column vector, every image can be regarded as a vector with a dimension of $n \times n$.

2.2. Dimensionality Reduction

1) Background of ISOMAP Algorithm: ISOMAP algorithm is one of manifold

learning algorithms, which is a nonlinear data dimensionality reduction method that has developed in recent years. Its main idea is to find low-dimensional manifold structures from high-dimensional data, that is to find low-dimensional manifolds in high-dimensional space, in order to achieve dimensionality reduction or data visualization.

ISOMAP was first proposed by Tenenbaum *et al.* in the famous Science journal [14], which is a global property preserving manifold learning algorithm, and its low dimensional embedding results can reflect the geodesic distance on the manifold where the high dimensional observation samples are located [15]. So far, ISOMAP algorithm has been applied in many fields. For example, the algorithm has been applied to facial expression recognition in [16], as well as to face recognition in [17] or classification in [18] or wireless sensor network positioning in [19], which reflects the practicability of the algorithm.

2) ISOMAP Algorithm: As mentioned earlier, after the features of an image are extracted, we obtain a column vector. The dimension of this column vector is determined by the dimension of the gray value matrix of the image. Assume that we have completed the feature extraction of the data set, and the extracted features are formed into a matrix $\mathcal{X} = \{x_1, x_2, \dots, x_N\}$. The dimensionality of any x_i is D . Note that x_0 is a point to be identified. The specific steps for recognizing oracle bone script with ISOMAP algorithm are listed here.

- Neighborhood definition. The neighborhood of X_i in dataset can be constructed by either its k -neighborhood or ϵ -neighborhood [20].
- Compute the Euclidean distance matrix D . The matrix can be calculated by

$$D = [d(x_i, x_j)] \quad (1)$$

$$d_{ij}^2 = (x_i - x_j)'(x_i - x_j). \quad (2)$$

- Calculate geodesic distance matrix G . The matrix of geodesic distance G can be calculated by the shortest path distance between any two sample points, that is

$$G = [g(x_i, x_j)] \quad (3)$$

$$g(x_i, x_j) = \min(d_{ij}, d_{il} + d_{lj}). \quad (4)$$

- Computes low-dimensional embedding $Y = \{y_1, y_2, \dots, y_N\}$. After calculating the matrix G , low-dimensional embedding is obtained by inputting G to MDS algorithm.

2.3. Method of Recognition

In this paper, in order to solve the problem of edge points which close to other species, we select the result of decision recognition according to the number of points of the nearest category. The label corresponding to N points is classified into C_1, C_2, \dots, C_M , and find the maximum of them by

$$C_j = \max\{C_1, C_2, \dots, C_M\}. \quad (5)$$

Finally, we take the label corresponding to the minimum value in C_j as the final identification result. In other words, if the number of points of the some types closest to the test point to be measured is the largest, the point of the type closest to the test point to be measured is selected as the final recognition result. If the closest points are multiple, they are C_1, C_2, \dots, C_p . Then the minimum Euclidean distance of every category d_1, d_2, \dots, d_p correspondence to C_1, C_2, \dots, C_p needs to be found, where p is the number of maximum types of points nearest to test point. Finally, the final recognition result is

$$\hat{d}_m = \min \{ \hat{d}_1, \hat{d}_2, \dots, \hat{d}_p \}. \tag{6}$$

The Corresponding label of \hat{d}_m is judged to be the closest image.

From the previous description, the method for recognizing the image of oracle bone script can be written as

- Identify the point x_0 . Calculate Euclidean distance \hat{d}_i between every x_i and x_0 by

$$\hat{d}_i^2 = \hat{d}^2 (y_i, y_0) = (y_i - y_0)' (y_i - y_0). \tag{7}$$

We take the first N minimum \hat{d}_i , and the labels corresponding to y_i in \hat{d}_i are divided into M categories. The maximum number of labels C_1, C_2, \dots, C_M corresponding to each category is calculated separately. Finally, we calculate C_j by

$$C_j = \max \{ C_1, C_2, \dots, C_M \}, \tag{8}$$

where C_j is a type of sample points which closest to x_0 . We take the label corresponding to the minimum \hat{d}_p value in C_j as the final recognition result.

3. Simulation Experiments

3.1. Experimental Condition

1) Selection of Samples: In this paper, the opening dataset of OBC306 is selected as dataset. There are 6 kinds of images which selected from the dataset, as shown in **Figure 4**.

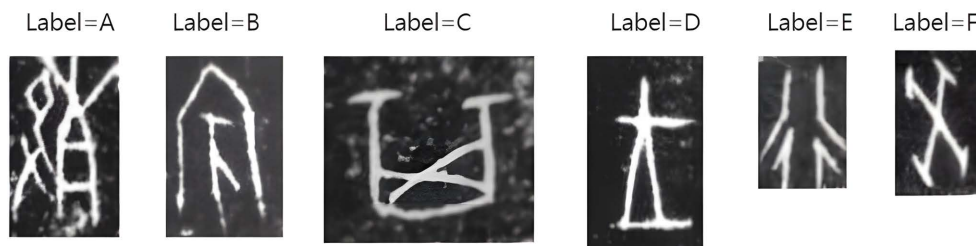


Figure 4. Partial images from the dataset, and corresponding labels to them.

Although only one image from each category is shown here, in fact, each category is made up of 20 identical type images. A sample set composed of 120 images was obtained.

Algorithm 1 ISOMAP algorithm

Input : A matrix of sample data: $(\mathbf{x}_1, \mathbf{x}_2, \dots, \mathbf{x}_N) \subseteq \mathcal{X} \subseteq \mathbb{R}^{D \times N}$.

- 1: **If** $\mathbf{d}_{ij} > \epsilon$
- 2: There exist edge connection.
- 3: **Else**
- 4: There is no edge connection, and $\mathbf{d}_{ij} = +\infty$.
- 5: **End if**
- 6: **While** $\mathbf{d}_{ij} > \epsilon$
- 7: Compute \mathbf{D} by using Eq.2.
- 8: **End while**
- 9: Compute \mathbf{G} by using Eq.4.
- 10: Enter \mathbf{G} into MDS algorithm.
- 11: Calculate \mathbf{d}_i and \mathbf{C}_j by using Eq.5 and Eq.6.
- 12: Find the label corresponding to $\hat{\mathbf{d}}_p$ in \mathbf{C}_j .
- 13: **End**

Output : A label corresponding to minimum. $\hat{\mathbf{d}}_p$

2) Sample Set Preprocessing: After the sample set is determined, we denoise the image by means of gray value adjustment, and then carry out size normalization. In **Figure 5**, the image was normalized the size as 128×128 and saved in BMP format on computer.

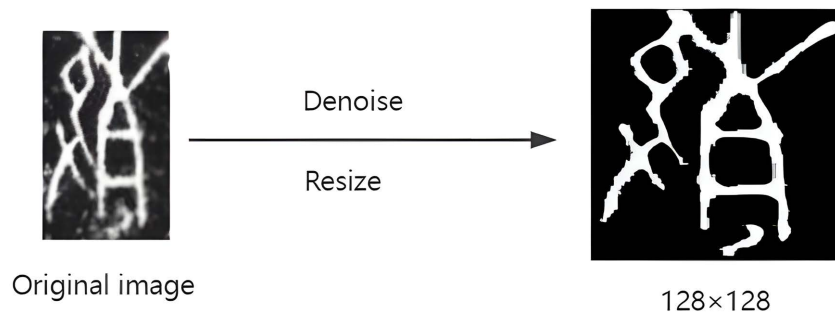


Figure 5. Preprocessing of a certain image.

Therefore, the dimension of the gray value matrix of every image is 128×128 , and finally we concatenate the gray value matrix columns into a column vector, the dimension is 128×128 .

3) Parameter Setting: The value of ϵ -neighborhood is obtained through the Euclidean distance matrix calculated by Equation (2) The distance in the distance matrix of all sample sets ranges from 21,000 to 31,000. To make sure that the adjacency graph is connected, the first small value of ϵ -neighbor should be determined through adding $20\% \delta$ to the minimum distance, where $\delta = 31000 - 21000$. Similarly, the n -th small value of ϵ -neighbor is determined through adding $20\% n \delta$ ($n = 2, \dots, 5$) to the minimum distance. We set 23,000, 25,000, 27,000, 29,000, and 31,000 as the value of different ϵ -neighborhood, respectively. To visualize high-dimensional data, the value of embedding dimension d is set to 3. To evaluate the impact of dimensionality, the d is set to 15, 35, 55,

75, and 95 in this study, respectively. The number of the nearest neighbors of the test point is set to $N = 1, 3, 7, 13, 19$ for the 6 different sample sets, respectively.

3.2. Experiment Results

The low-embedding of dimensional reduction is obtained by using ISOMAP algorithm on sample set. Then the low-dimension vector is displayed in a 3-dimensional coordinate system, which is shown as follows.

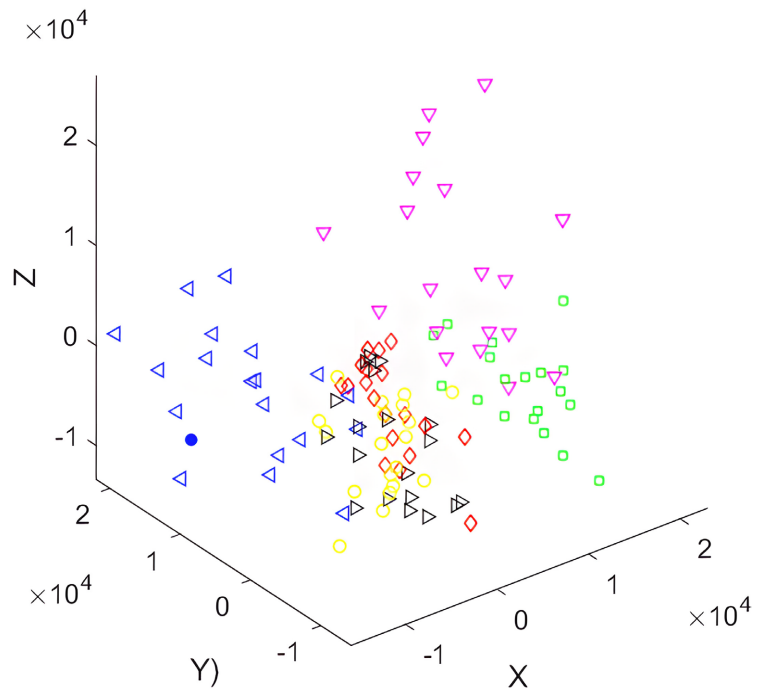


Figure 6. Sample set visualized by using ISOMAP algorithm.

In **Figure 6**, the parameter of ϵ -neighborhood is 29,000. The different colored points represent different categories, and deepened points represent to be identified.

Through many trials, the average accuracy rate was obtained when the ϵ neighborhoods and the N were set in different values. The experimental results are shown in **Table 1**.

Table 1. The average accuracy of different values of ϵ -neighborhood under various values of N , where N refers to the number of the nearest neighbors of the test point.

	$\epsilon = 23000$	$\epsilon = 25000$	$\epsilon = 27000$	$\epsilon = 29000$	$\epsilon = 31000$
$N = 1$	62.5%	60.8%	72.5%	88.3%	77.6%
$N = 3$	66.7%	67.5%	70.8%	85.8%	85.0%
$N = 7$	66.7%	66.7%	78.3%	93.3%	90.0%
$N = 13$	60.8%	69.2%	72.5%	91.7%	87.5%
$N = 19$	60.8%	62.5%	69.1%	89.1%	92.5%

From the table, we can observe that when the neighborhood is taken as $\epsilon = 29000$ and $N = 7$, the recognition accuracy reaches 93.3%, which is the best recognition rate under these parameters. In order to observe the impact of changes in N on the average accuracy, a line graph was plotted to show the effect of varying values of N on the recognition rate, as illustrated in **Figure 7**.

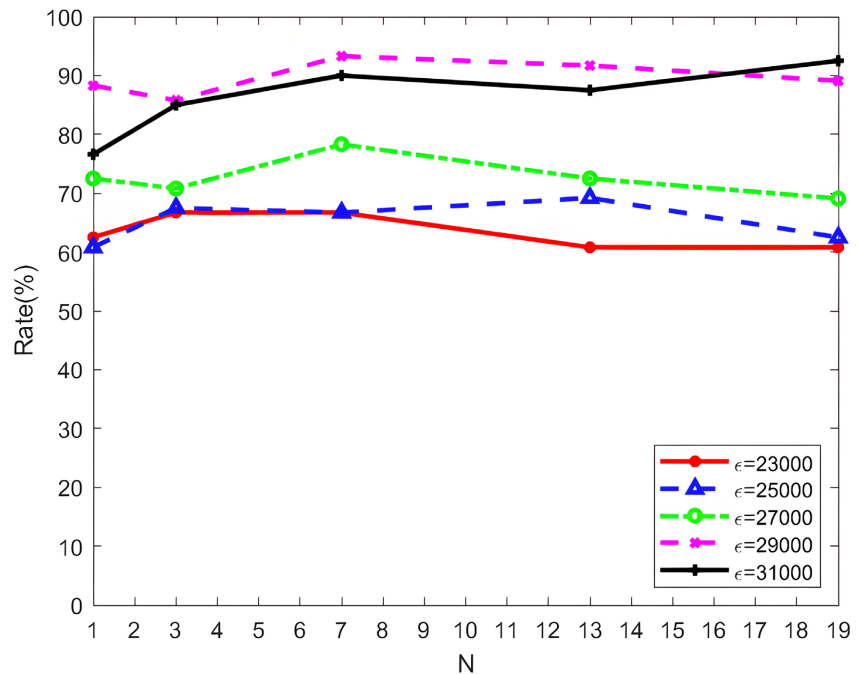


Figure 7. The average accuracy of different values of ϵ -neighborhood under various values of N , where N refers to the number of the nearest neighbors of the test point.

It can be observed that as N increases, the accuracy shows an increasing trend. When N reaches a certain value, the recognition rate reaches its optimum and gradually begins to decline. As we can intuitively see in the figure, when the value of $N = 7$ and $\epsilon = 29000$, the optimal recognition rate under this parameter can be achieved. This experiment indicates that selecting larger neighbors in the algorithm can achieve a better recognition rate. This is because choosing larger neighboring points can capture the features at sample points and also reduce the introduction of noise.

A large number of experiments are conducted with study, the impact of the embedding dimension and the ϵ -neighbor on the average recognition rate, as shown in **Figure 8**.

It can be observed that a large value of ϵ -neighborhood consistently achieves superior recognition rate compared to the small values. This is because a large value of ϵ -neighborhood can capture more discriminative structural features than a small value. It can also be seen that the average accuracy rate tends to decline gradually as the dimension increases. This can be attributed to the introduction of noise components in high-dimensional manifolds, which induces erroneous classifications. Notably, when the embedding dimension exceeds a critical threshold

(approximately when $d > 55$ in this study), the mean recognition accuracy demonstrates asymptotic stabilization. This result reveals that with the increase in dimension, the average recognition rate tends to be stabilized and exhibits better robustness under higher embedding dimensions.

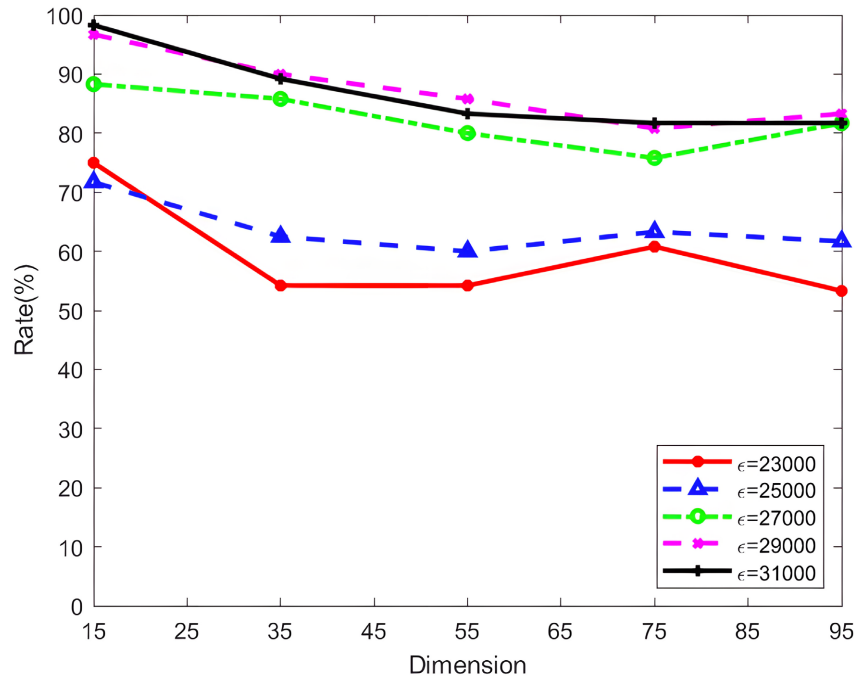


Figure 8. The average accuracy of different values of ϵ -neighborhood under various values of embedding dimension.

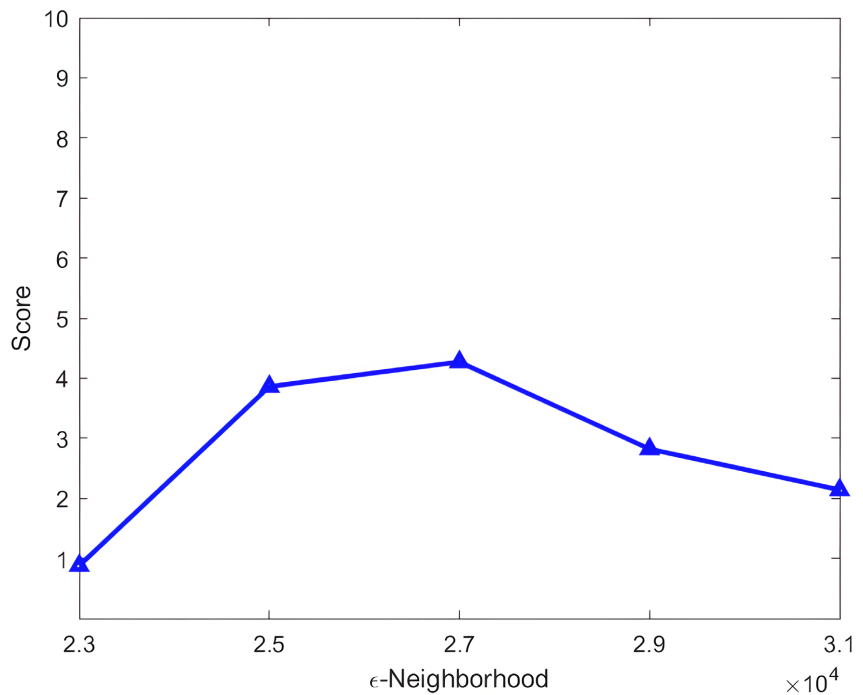


Figure 9. Robustness scores under different ϵ -neighborhoods.

To evaluate the parametric robustness of the algorithm through adjusting the value of neighborhood, we formulate a stability metric which refers to the robustness score. It is obtained through formulating the ratio of the average recognition rate to the standard deviation. The results of extensive experiments are presented in **Figure 9**.

It can be observed that the curve shows a trend of rising first and then falling with the increase of ϵ -neighbor. Notably, the results indicate that when $\epsilon = 27000$, the experimental results exhibit the best robustness. This is because a small value of ϵ -neighbors cannot remain the local structures of the algorithm. While a large value of neighbors leads to the introduction of noise. So it is very important to find a suitable value to maintain the balance between local structure and global structure.

Usually, the efficiency of one algorithm can be reflected by its time cost. To demonstrate the efficiency of this algorithm in recognizing oracle bone inscriptions images, we recorded the running time of tests with different numbers of samples n , and $n = 100, 200, 400, 600, 800$. The recorded results are illustrated in **Figure 10**.

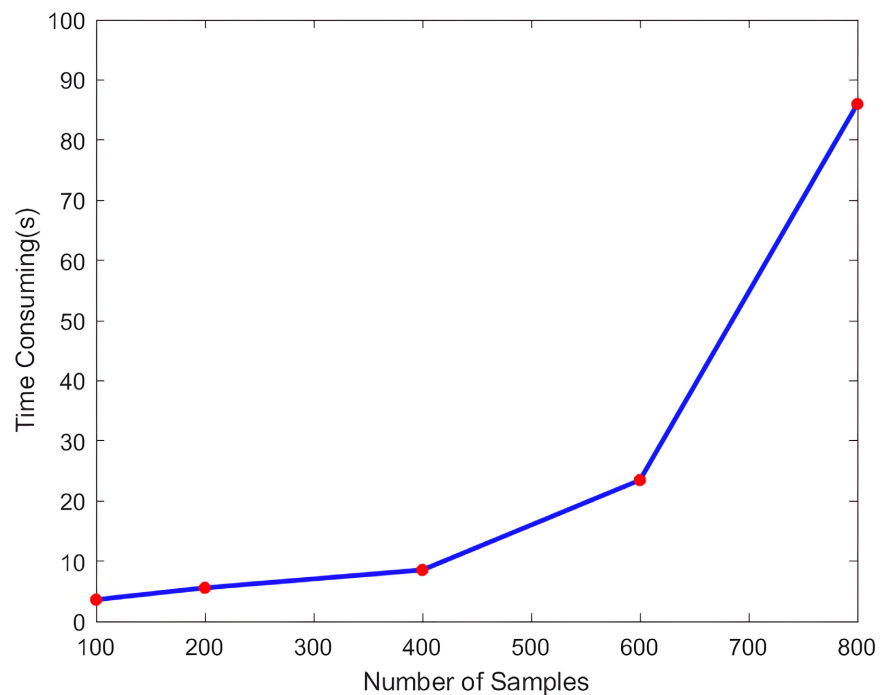


Figure 10. Time consumption for different numbers of samples.

It can be observed that as the sample size increases, the time shows an exponential growth trend. The time cost is 5 seconds when we have 100 samples, while it is 86 seconds when we have 800 samples. The results indicate that the algorithm can be directly executed on small-scale datasets. While dealing with large-scale data, it is necessary to introduce approximate computation strategies that reduce the number of shortest paths to reduce time consumption.

3.3. Comparison with Other Algorithms

In order to compare the advantages of this algorithm, we apply several other algorithms of manifold learning algorithm as a comparison reference in the paper. We also obtain the low dimensional embedding of different algorithms at same sample set, which are shown in **Figures 11-13**.

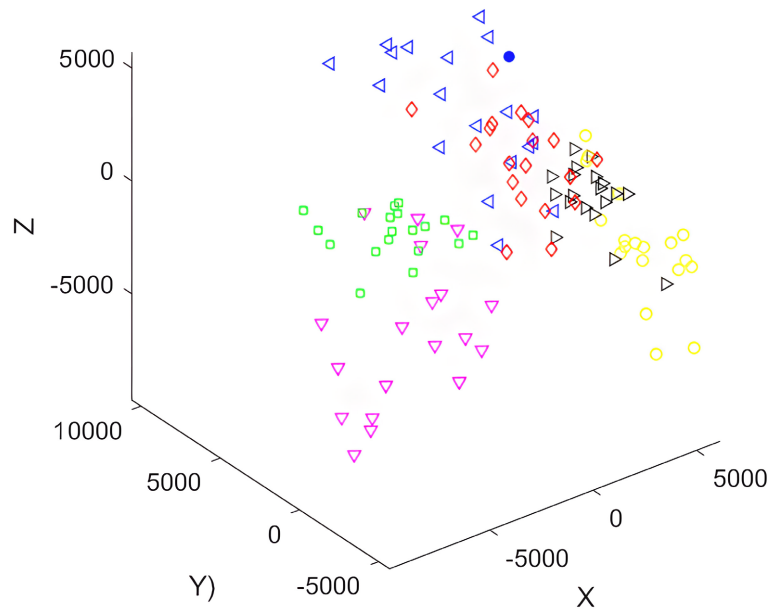


Figure 11. Sample sets visualized by using MDS algorithm.

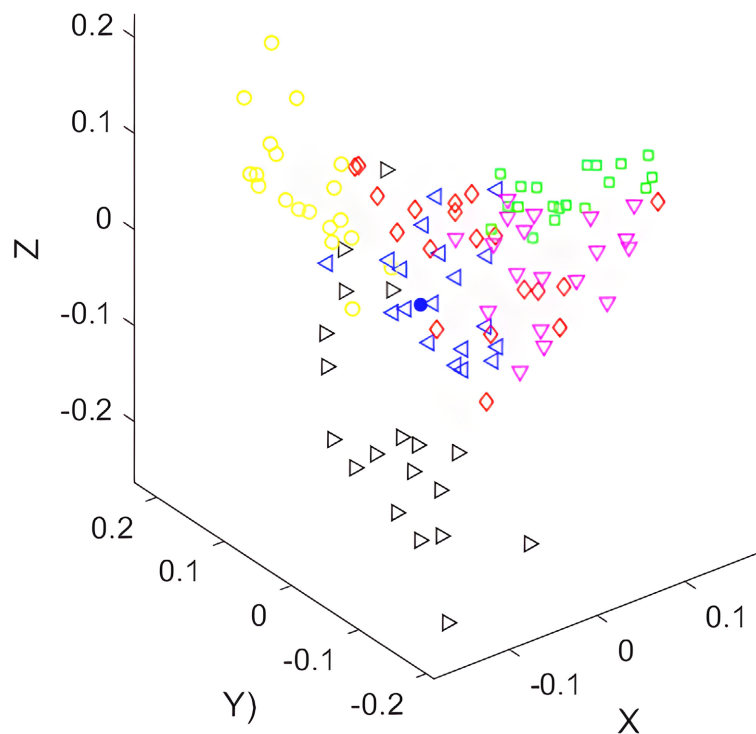


Figure 12. Sample sets visualized by using LLE algorithm.

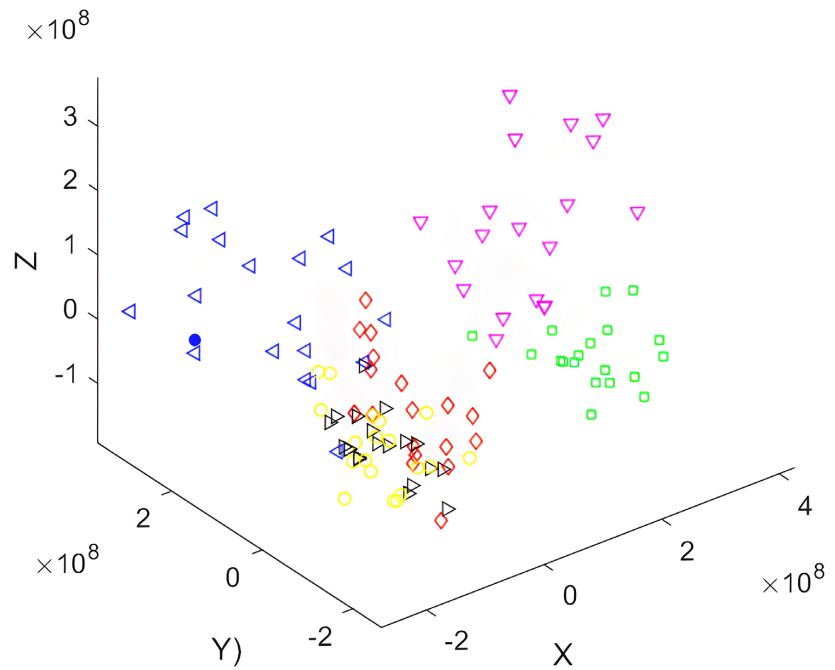


Figure 13. Sample sets visualized by using PCA algorithm.

Similarly, we get the average accuracy rate of the responding algorithm in **Figure 14** and **Figure 15**.

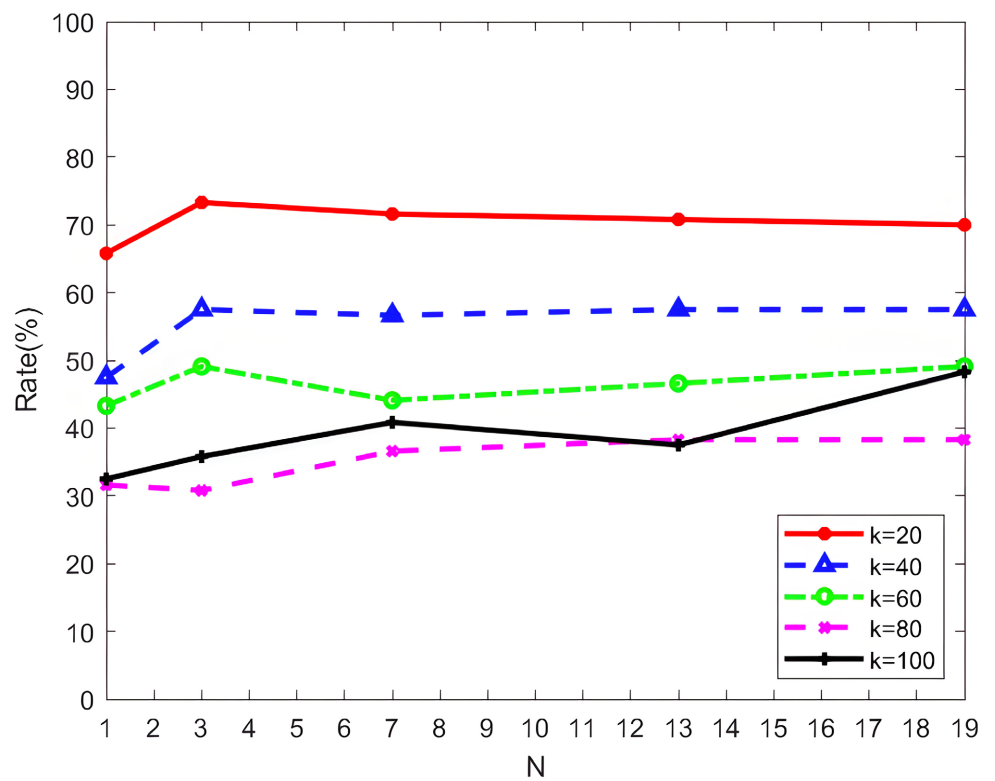


Figure 14. The average accuracy of different numbers of k -nearest neighbors under various values of N , where N refers to the number of the nearest neighbors of the test point.

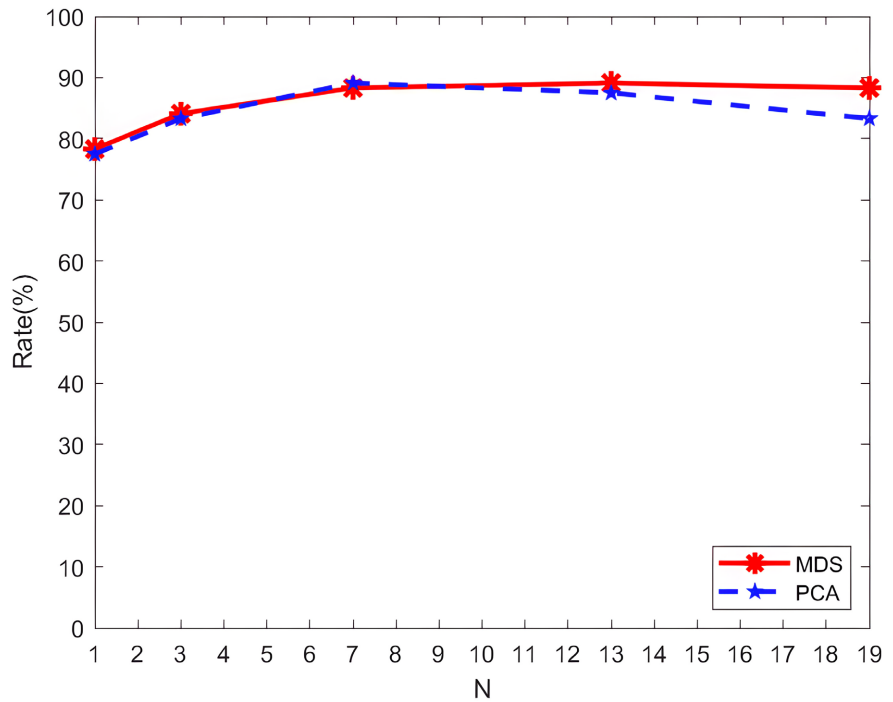


Figure 15. The average accuracy of different algorithms under various values of N , where N refers to the number of the nearest neighbors of the test point.

According to the experimental data, we obtain the optimal accuracy rate and time-consuming of all manifold learning algorithms to recognize the images, which are shown as follows.

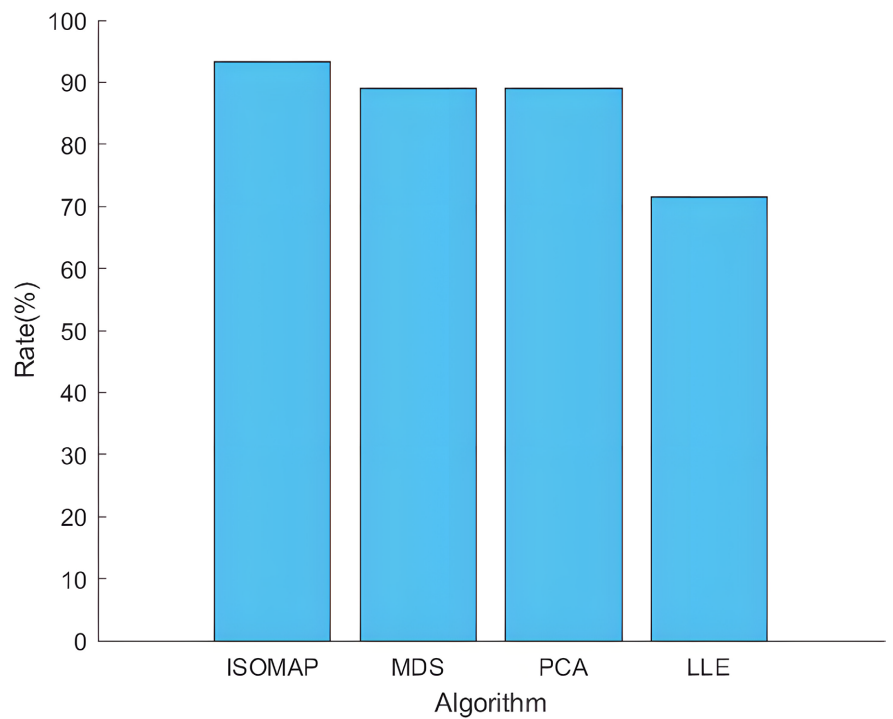


Figure 16. The mean average accuracy of different algorithms.

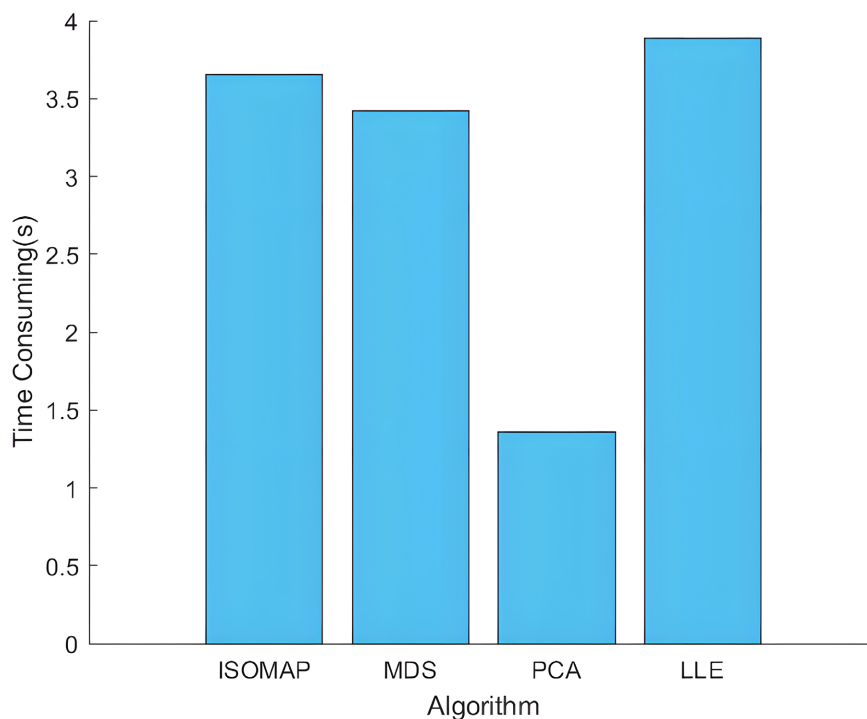


Figure 17. The time-consuming of different algorithms.

In **Figure 16**, it can be observed that the ISOMAP dimensionality reduction algorithm has a significant advantage in the average recognition rate. This is because the method effectively maintains the geodesic distances of the sampling points in high-dimensional space after dimensionality reduction, thereby preserving the nonlinear characteristics of the data. From **Figure 17**, it can be concluded that the time taken by the ISOMAP algorithm is relatively slow, being only faster than the LLE algorithm. This is due to the high computational complexity of ISOMAP algorithm, which requires more time and resources. We can conclude that although the ISOMAP algorithm has certain disadvantages in terms of time consumption, its performance advantages allow it to recognize images more accurately, which is exactly what we expect.

In the experiment, the low-dimensional embeddings of the sample set were first calculated using the ISOMAP algorithm. Subsequently, the results of the low-dimensional embeddings were visualized and analyzed for the effects of dimensionality, indicating that the algorithm demonstrates a better recognition rate at lower dimensions. Next, we investigated the impact of parameter N on recognition accuracy under different neighbors, obtaining the average recognition rates under various parameters after multiple experiments, and compared these results with those of the PCA, MDS, and LLE algorithms. Finally, we analyzed and compared the experimental results, where the ISOMAP algorithm achieved the best recognition rate of 93.3%. Although the ISOMAP algorithm has certain disadvantages in terms of running time, its performance advantage in recognition accuracy allows it to effectively complete the recognition task.

4. Conclusion

This paper employs the ISOMAP algorithm to identify oracle bone inscription images. The recognition process includes five steps: sample set selection, image preprocessing, feature extraction, dimensionality reduction, and classification. Experimental results indicate that, compared to MDS, PCA, and LLE algorithms, ISOMAP exhibits better performance in terms of average recognition rate and computational efficiency. Therefore, ISOMAP can be considered an effective method for accurately identifying oracle bone inscription images. However, the algorithm remains highly sensitive to noise and currently cannot handle incomplete images. Future work will focus on enhancing its noise resistance and robustness to achieve broader applicability.

Disclosure Statement

No potential of interest was reported by the authors.

Supported

This subject is supported by the National Natural Science Foundation of China (No. 12001439).

Conflicts of Interest

The authors declare no conflicts of interest regarding the publication of this paper.

References

- [1] Fu, X., Yang, Z., Zeng, Z., Zhang, Y. and Zhou, Q. (2022) Improvement of Oracle Bone Inscription Recognition Accuracy: A Deep Learning Perspective. *ISPRS International Journal of Geo-Information*, **11**, Article 45. <https://doi.org/10.3390/ijgi11010045>
- [2] Keightley, D.N. (1979) The Shang State as Seen in the Oracle-Bone Inscriptions. *Early China*, **5**, 25-34. <https://doi.org/10.1017/s0362502800006118>
- [3] Huang, S., Wang, H., Liu, Y., Shi, X. and Jin, L. (2019) OBC306: A Large-Scale Oracle Bone Character Recognition Dataset. 2019 *International Conference on Document Analysis and Recognition (ICDAR)*, Sydney, 20-25 September 2019, 681-688. <https://doi.org/10.1109/icdar.2019.00114>
- [4] Cheung, C. (2018) The Chinese History That Is Written in Bone. *American Scientist*, **106**, 133-134. <https://doi.org/10.1511/2018.106.3.133>
- [5] Song, Z. (2016) Collection of Oracle Bone Rubbings of Hu. Shanghai Ancient Books Publishing House.
- [6] Wang, L., Wang, C.J. and Jiao, Q.J. (2023) Research on Handwriting Oracle Recognition Based on EasyDL. *Electronic Technology and Software Engineering*, **3**, 184-187.
- [7] Feng, Y. (1996) Recognition of Jia Gu Wen Based on Graph Theory. *Journal of Electronics and Information Technology*, **18**, 41-47.
- [8] Lu, X., Li, M., Cai, K., et al. (2010) A Graphic-Based Method for Chinese Oracle-Bone Classification. *Journal of Beijing Information Science or Technology University*, **25**,

92-96.

- [9] Chua, L.O. (1997) CNN: A Vision of Complexity. *International Journal of Bifurcation and Chaos*, **7**, 2219-2425. <https://doi.org/10.1142/s0218127497001618>
- [10] Liu, G. (2018) Oracle-Bone Inscription Recognition Based on Deep Convolutional Neural Network. *Journal of Computers*, **8**, 1442-1450. <https://doi.org/10.17706/jcp.13.12.1442-1450>
- [11] Meng, L., Kamitoku, N. and Yamazaki, K. (2018) Recognition of Oracle Bone Inscriptions Using Deep Learning Based on Data Augmentation. 2018 *Metrology for Archaeology and Cultural Heritage (MetroArchaeo)*, Cassino, 22-24 October 2018, 33-38. <https://doi.org/10.1109/metroarchaeo43810.2018.9089769>
- [12] Chen, T., Qian, Y., Pei, J., Wu, S., Wu, J., Li, L., *et al.* (2020) A Study on Encoding-Based Oracle Bone Script Recognition. *Journal of Chinese Writing Systems*, **4**, 281-290. <https://doi.org/10.1177/2513850220952890>
- [13] Liu, Y.G. and Liu, G.Y. (2017) Oracle Bone Inscription Recognition Based on SVM. *Journal of Anyang Normal University*, **2**, 54-56.
- [14] Tenenbaum, J.B., Silva, V.D. and Langford, J.C. (2000) A Global Geometric Framework for Nonlinear Dimensionality Reduction. *Science*, **290**, 2319-2323. <https://doi.org/10.1126/science.290.5500.2319>
- [15] Xu, H. (2017) The Methods of Information Geometry in Wireless Sensor Networks. Ph.D. Thesis, Beijing Institute of Technology.
- [16] Zhao, X. and Zhang, S. (2011) Facial Expression Recognition Based on Local Binary Patterns and Kernel Discriminant Isomap. *Sensors*, **11**, 9573-9588. <https://doi.org/10.3390/s111009573>
- [17] Liu, J., Wang, H., Zhou, X. and Luo, F. (2013) Face Recognition Based on Improved Isometric Feature Mapping Algorithm. *Journal of Computer Applications*, **33**, 76-79. <https://doi.org/10.3724/sp.j.1087.2013.00076>
- [18] Weng, X. and Qin, S. (2012) Classification of Multivariate Time Series Using Supervised Isomap. 2012 *Third Global Congress on Intelligent Systems*, Wuhan, 6-8 November 2012, 136-139. <https://doi.org/10.1109/gcis.2012.31>
- [19] Yang, H. and Li, B. (2019) Node Localization of Wireless Sensor Network Based on the Kernel Matrix ISOMAP Algorithm. *Journal of East China Normal University*, **9**, 115-123.
- [20] Wang, J. (2012) Geometric Structure of High-Dimensional Data and Dimensionality Reduction. Higher Education Press.